

# Electromagnetic calorimetry requirements from flavour physics for application at FCC-ee

---

**Lars Röhrig,<sup>a,b</sup> Stéphane Monteil<sup>b</sup>**

*<sup>a</sup>Department of Physics, TU Dortmund University, Dortmund, Germany*

*<sup>b</sup>Université Clermont-Auvergne, CNRS, LPCA, 63000 Clermont-Ferrand, France*

*E-mail:* [lars.roehrig@tu-dortmund.de](mailto:lars.roehrig@tu-dortmund.de)

**ABSTRACT:** This technical note reports an academic exercise to assess the electromagnetic (EM) calorimeter energy resolution performance that would be needed in order to separate candidates of the radiative quark transitions  $b \rightarrow s\gamma$  and  $b \rightarrow d\gamma$ .

---

## Contents

<b>1</b>	<b>Physics motivations</b>	<b>1</b>
<b>2</b>	<b>Detector requirements</b>	<b>2</b>
<b>3</b>	<b>Analysis</b>	<b>2</b>

---

## 1 Physics motivations

The study of radiative decays, such as  $B_d^0 \rightarrow K^* \gamma$  ( $b \rightarrow s \gamma$ ) and  $B_s^0 \rightarrow K^* \gamma$  ( $b \rightarrow d \gamma$ ), serves as an important test of the Standard Model of Particle Physics (SM). Furthermore, it is a sensitive probe for potential Beyond the SM (BSM) effects in one-loop penguin diagrams [1–3], as flavour-changing neutral current (FCNC) processes are forbidden at tree level in the SM. New heavy particles can enter the loop diagrams, altering the decay amplitudes and observables such as branching fractions, mixing-induced charge-parity ( $CP$ ) asymmetries, and polarisation fractions. Examples of  $b \rightarrow s \gamma$  and  $b \rightarrow d \gamma$  transitions for both decays are shown in Fig. 1.



**Figure 1:**  $b \rightarrow s \gamma$  and  $b \rightarrow d \gamma$  at quark level in the SM.

Moreover, the amplitudes for  $B_d^0 \rightarrow K^* \gamma$  and  $B_s^0 \rightarrow K^* \gamma$  are proportional to the elements of the Cabibbo-Kobayashi-Maskawa (CKM) matrix, allowing to place constraints to the unitarity triangle profile complementary to those of the oscillation frequencies. At a possible next-generation circular lepton collider such as the Future Circular Collider as an electron-positron accelerator (FCC-ee) [4], approximately

$$N_{B_d^0} \approx N_Z \cdot P(Z \rightarrow \text{hadrons}) \cdot R_b \cdot f_{b \rightarrow B_d^0} \cdot \text{Br}(B_d^0 \rightarrow K^* \gamma) \approx 30 \cdot 10^6. \quad (1.1)$$

will be produced following In Eq. (1.1),  $N_Z = 6 \cdot 10^{12}$  events are foreseen at the  $Z$  pole at a centre-of-mass energy of  $\sqrt{s} = m_Z$ . The remaining inputs are

$$\begin{aligned} P(Z \rightarrow \text{hadrons}) &\approx 0.7 \text{ [5]}, & R_b &= 0.216 \text{ [5]}, \\ f_{b \rightarrow B_d^0} &\approx 0.4 \text{ [6]}, & \text{Br}(B_d^0 \rightarrow K^* \gamma) &= 4.18 \cdot 10^{-5} \text{ [5]}. \end{aligned}$$

The  $B_s^0 \rightarrow K^* \gamma$  decay, unobserved to date, is one example of  $b \rightarrow d$  transitions that FCC-ee can probably uniquely study, if it can benefit from an accurate photon-energy measurement complementing the already established exquisite reconstruction of displaced vertices.

## 2 Detector requirements

A key aspect of studying  $B_{d,s}^0 \rightarrow K^* \gamma$  decays is the reconstruction and differentiation of both modes that share a common final state. Several detector concepts are currently under active discussion. The one used in this study is the IDEA detector concept [7, 8]. It consists of a silicon vertex detector positioned near the beam pipe, a drift chamber for an almost continuous tracking of charged particles, and a dual-readout calorimeter to measure electromagnetic and hadronic showers of interacting particles. The photon-energy resolution is the critical parameter when it comes to distinguishing the  $B_d^0$  from the  $B_s^0$  decay. The energy resolution provided by the dual-readout calorimeter is assumed to be of the order  $12\%/\sqrt{E_\gamma}$ , while alternative concepts based on crystals (see, *e.g.* Ref. [9]) could provide energy resolutions of the order  $\mathcal{O}(2\%/\sqrt{E_\gamma})$ . In the following analysis, which is meant more as an academic exploration than a physics sensitivity study, the importance of the photon-energy resolution for flavour physics is highlighted.

## 3 Analysis

The analysis is based on about  $30 \cdot 10^6$  privately produced event samples, where the  $B_d^0 \rightarrow K^* \gamma$  decay has been exclusively generated with PYTHIA8 [10] and EvtGen [11]. The detector response has been modelled using the IDEA card from the DELPHES [12] software package. The reconstruction has been seeded with Monte-Carlo (MC) information, and no background processes have been considered, since the goal is to derive requirements for the photon-energy resolution in the electromagnetic calorimeter. For this purpose, the  $K^*$  has been reconstructed from a charged kaon and pion, while the photon energy  $E_\gamma^{\text{MC}}$  has been taken from the corresponding MC photon. Furthermore, a reconstruction efficiency of 100 % has been assumed. The smeared photon-energy response has then been drawn from a Normal distribution  $\mathcal{N}(\mu, \sigma)$  with mean  $\mu$  and standard deviation  $\sigma$  via

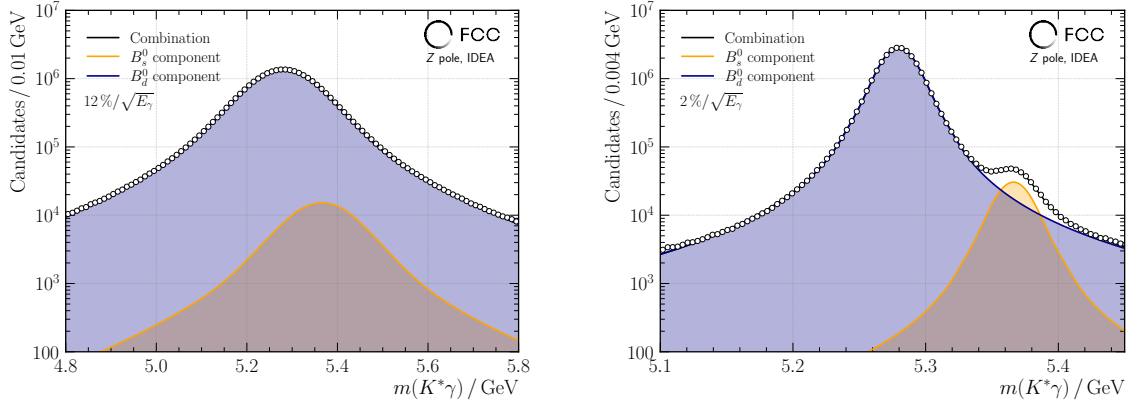
$$E_\gamma^{\text{smeared}} = \mathcal{N}\left(E_\gamma^{\text{MC}}, r \cdot \sqrt{E_\gamma^{\text{MC}}}\right). \quad (3.1)$$

In Eq. (3.1) the resolution of the stochastic term  $r$  given in percentage units. It has been validated that a value of  $r \approx 0.12$  corresponds to the energy resolution of the dual-readout calorimeter, which is used by default in the IDEA detector concept. From  $E_\gamma^{\text{smeared}}$ , the momentum components of the photon have been recalculated using angular relations

$$\begin{aligned} \theta &= \frac{p_z^{\text{MC}}}{E_\gamma^{\text{MC}}}, \\ \phi &= \arctan2(p_y^{\text{MC}}, p_x^{\text{MC}}). \end{aligned} \quad (3.2)$$

From these, the recalculated momentum components result to

$$\begin{aligned} p_x^{\text{smeared}} &= E_\gamma^{\text{smeared}} \cdot \sin(\theta) \cos(\phi), \\ p_y^{\text{smeared}} &= E_\gamma^{\text{smeared}} \cdot \sin(\theta) \sin(\phi), \\ p_z^{\text{smeared}} &= E_\gamma^{\text{smeared}} \cdot \cos(\theta). \end{aligned} \quad (3.3)$$



(a) IDEA baseline scenario with a dual-readout calorimeter,  $r = 0.12$ .

(b) High photon-energy resolution from crystals,  $r = 0.02$ .

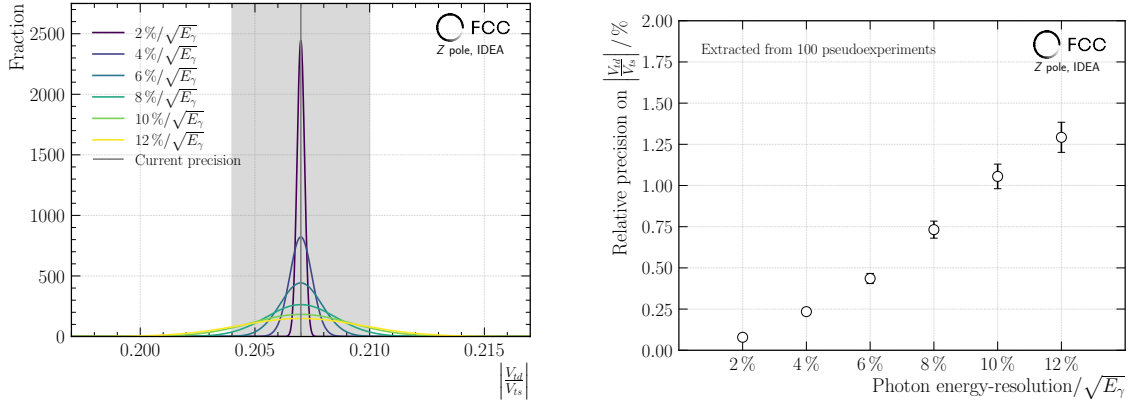
**Figure 2:** Two distributions of the invariant  $K^*\gamma$  mass, where almost no  $B_s^0$  signal can be observed on the right side. With a high photon-energy resolution with  $r = 0.02$ , even angular analyses are in reach due to the clear signal peak in the mass spectrum. In both cases, the interpolated functions describe the spectrum well.

For the sake of this study, the  $B_s^0$  signal yield has been estimated from the CKM matrix elements and the corresponding hadronisation fractions  $f_{b \rightarrow B_d^0} = 0.4$  and  $f_{b \rightarrow B_s^0} = 0.1$  via

$$\frac{N_{B_d^0}}{N_{B_s^0}} \sim \frac{f_{b \rightarrow B_d^0}}{f_{b \rightarrow B_s^0}} \cdot \left| \frac{V_{ts}}{V_{td}} \right|^2 \approx 92. \quad (3.4)$$

Different photon-energy resolution scenarios have been assumed with  $r \in [0.12, 0.02]$  in increments of 0.02. The upper limit of this range is dictated by the fit convergence difficulties encountered when reaching high-values of the sampling resolution term, which are likely making the measurement with real data. The resulting invariant-mass distribution  $m(K^*\gamma^{\text{smearred}})$  has been modelled with a double-sided Crystal-Ball function in addition to a Gaussian core for each contribution  $B_d^0$  and  $B_s^0$ . The eight shape parameters have been extracted from an interpolation to only the  $B_d^0$  signal peak before extracting  $|V_{ts}/V_{td}|^2$  from an interpolation to the combined signal.

In Fig. 2, the left and right panels show the case for  $r = 0.12$  and  $r = 0.02$  (high photon-energy resolution from crystals; see also Ref. [9]). Only with a sufficiently high photon-energy resolution, the peak of the  $B_s^0$  signal becomes visible and distinguishable from the overwhelming  $B_d^0$  background. The purity in the latter case would even allow to perform studies of angular observables like the photon polarisation or of  $CP$  asymmetries in the decay rates of  $B_s^0$  and  $\bar{B}_s^0$  mesons. However, from the extracted event-yield ratio,  $|V_{td}/V_{ts}|$  as well as its uncertainty, have been examined. In order to spot biases in the fit, 100 toy experiments have been performed in order to extract the statistical uncertainty. For all photon-energy resolutions considered, no bias has been found and the resulting distributions have been fitted with a Gaussian distribution. These fits are shown in the left panel of Fig. 3, while the relative statistical uncertainty on  $|V_{td}/V_{ts}|$  are presented in the



(a) The Gaussian fits of the toy studies for the different photon-energy resolutions. (b) The relative precision as a function of the energy resolution.

**Figure 3:** The photon energy-resolution is the driving impact on the measurement precision of  $|V_{td}/V_{ts}|$ . Competitive results with respect to the current precision are in reach with all photon-energy resolutions under study.

right panel of the same figure as a function of the photon-energy resolution. In the figure, the current SM precision from  $|V_{td}/V_{ts}| = 0.207 \pm 0.003$  [5] is highlighted as a gray line.

As can be seen, with all photon-energy resolutions under study, competitive precisions on  $|V_{td}/V_{ts}|$  are in reach, even for  $12\%/\sqrt{E_\gamma}$ . However, several words of cautions are in order when it comes to the interpretation of this academic exercise. The focus of the study is centred onto the separation power of the two transitions  $b \rightarrow (d, s)\gamma$ . The study hence assumed perfect charged hadron particle and photon identification. Moreover, the physical backgrounds (*e.g.* the charmless transition  $B^0 \rightarrow K\pi\pi^0$  with the  $\pi^0$  is misidentified as a photon) are neglected. Last but not least, the fit procedure requires the knowledge of the signal shapes. It is obvious that mastering the tails is mandatory to make a valid measurement. It has been checked that the measurement is valid even with inaccurate signal shapes for the higher resolutions tested. By contrast, it is very likely that a slight bias in their knowledge would prevent to even perform the measurement for the worse energy resolutions considered in this study.

## References

- [1] S. Navas et al., *Review of particle physics*, Phys. Rev. D **110** (2024) 030001, DOI: [10.1103/PhysRevD.110.030001](https://doi.org/10.1103/PhysRevD.110.030001).
- [2] A. J. Buras, M. Misiak, M. Munz, and S. Pokorski, *Theoretical uncertainties and phenomenological aspects of  $B \rightarrow X(s) \gamma$  decay*, Nucl. Phys. B **424** (1994) 374, DOI: [10.1016/0550-3213\(94\)90299-2](https://doi.org/10.1016/0550-3213(94)90299-2), arXiv: [hep-ph/9311345](https://arxiv.org/abs/hep-ph/9311345).
- [3] David Atwood, Michael Gronau, and Amarjit Soni, *Mixing induced CP asymmetries in radiative B decays in and beyond the standard model*, Phys. Rev. Lett. **79** (1997) 185, DOI: [10.1103/PhysRevLett.79.185](https://doi.org/10.1103/PhysRevLett.79.185), arXiv: [hep-ph/9704272](https://arxiv.org/abs/hep-ph/9704272).

- [4] A. Abada et al., *FCC-ee: The Lepton Collider*, The European Physical Journal Special Topics **228** (2019) 261, DOI: [10.1140/epjst/e2019-900045-4](https://doi.org/10.1140/epjst/e2019-900045-4).
- [5] R. L. Workman et al., *Review of Particle Physics*, PTEP **2022** (2022) 083C01, DOI: [10.1093/ptep/ptac097](https://doi.org/10.1093/ptep/ptac097).
- [6] DELPHI Collaboration, *A measurement of the branching fractions of the b-quark into charged and neutral b-hadrons*, Physics Letters B **576** (2003) 29, ISSN: 0370-2693, DOI: <https://doi.org/10.1016/j.physletb.2003.09.070>.
- [7] M. Antonello, *IDEA: A detector concept for future leptonic colliders*, Nuovo Cim. C **43** (2020), ed. by G. D'Ambrosio and G. De Nardo 27, DOI: [10.1393/ncc/i2020-20027-2](https://doi.org/10.1393/ncc/i2020-20027-2).
- [8] Gabriella Gaudio, *The IDEA detector concept for FCCee*, PoS **ICHEP2022** (2022) 337, DOI: [10.22323/1.414.0337](https://doi.org/10.22323/1.414.0337).
- [9] Sergey Barsuk et al., *First characterization of a novel grain calorimeter: the GRAiNITA prototype*, Journal of Instrumentation **19** (2024) P04008, DOI: [10.1088/1748-0221/19/04/P04008](https://doi.org/10.1088/1748-0221/19/04/P04008).
- [10] Torbjörn Sjöstrand et al., *An introduction to PYTHIA 8.2*, Computer Physics Communications **191** (2015) 159, ISSN: 0010-4655, DOI: <https://doi.org/10.1016/j.cpc.2015.01.024>.
- [11] David J. Lange, *The EvtGen particle decay simulation package*, Nuclear Instruments and Methods in Physics Research Section A: Accelerators, Spectrometers, Detectors and Associated Equipment **462** (2001), BEAUTY2000, Proceedings of the 7th Int. Conf. on B-Physics at Hadron Machines 152, ISSN: 0168-9002, DOI: [https://doi.org/10.1016/S0168-9002\(01\)00089-4](https://doi.org/10.1016/S0168-9002(01)00089-4).
- [12] The DELPHES 3 Collaboration, *DELPHES 3: a modular framework for fast simulation of a generic collider experiment*, Journal of High Energy Physics **2014** (2014) 57, DOI: [10.1007/JHEP02\(2014\)057](https://doi.org/10.1007/JHEP02(2014)057).